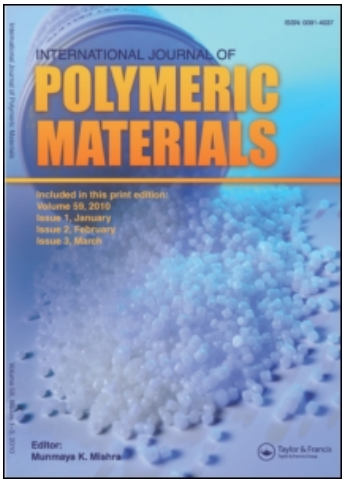

International Journal of Polymeric Materials
Publication details, including instructions for authors and subscription information:
http://www.informaworld.com/smpp/title~content=t713647664

Influence of Processing Conditions on the Properties of Polystyrene (PS)/organomontmorillonite (OMMT) Nanocomposites Prepared via Solvent Blending Method

S. V. Krishna[a]; G. Pugazhenthi[a]
[a] Department of Chemical Engineering, Indian Institute of Technology Guwahati, Guwahati, Assam, India

Online publication date: 03 January 2011

To cite this Article Krishna, S. V. and Pugazhenthi, G.(2011) 'Influence of Processing Conditions on the Properties of Polystyrene (PS)/organomontmorillonite (OMMT) Nanocomposites Prepared via Solvent Blending Method', International Journal of Polymeric Materials, 60: 2, 144 — 162
To link to this Article: DOI: 10.1080/00914037.2010.504167
URL: http://dx.doi.org/10.1080/00914037.2010.504167

International Journal of Polymeric Materials, 60:144–162, 2011

ISSN: 0091-4037 print/1563-535X online
DOI: 10.1080/00914037.2010.504167

Taylor & Francis
Taylor & Francis Group

Influence of Processing Conditions on the Properties of Polystyrene (PS)/ organomontmorillonite (OMMT) Nanocomposites Prepared via Solvent Blending Method

S. V. Krishna and G. Pugazhenthi

Department of Chemical Engineering, Indian Institute of Technology Guwahati, Guwahati, Assam, India

A series of polystyrene (PS)/organomontmorillonite (OMMT) clay nanocomposites was prepared by effectively dispersing the inorganic nanolayers of OMMT clay in the organic PS matrix via the solvent blending method using xylene as a solvent. The resulting samples were characterized using X-ray diffraction (XRD), scanning electron microscopy (SEM), transmission electron microscopy (TEM), Fourier transform infrared (FTIR) spectroscopy, thermogravimetric analysis (TGA), and differential scanning calorimetry (DSC). The XRD and TEM results show that the intercalation/exfoliation of OMMT can be divided into solvent swelling and layer breaking processes and is affected by several reaction parameters such as nanofiller loading, refluxing temperature, and refluxing time. TGA data show that the PS/OMMT nanocomposites have significant enhanced thermal stability. When 50% weight loss is selected as a point of comparison, the thermal decomposition temperature of PS/OMMT nanocomposite with 7 wt% of OMMT is 15°C higher than that of pure PS. The glass transition temperature (T_g) of PS/OMMT nanocomposites is about 5.0–6.2°C higher than that of pure PS. The water uptake capacity of PS/OMMT nanocomposites is negligible when compared with pure PS.

Keywords MMT, nanocomposites, polystyrene, solvent blending, thermal stability

Received 15 March 2010; accepted 2 June 2010.
Address correspondence to G. Pugazhenthi, Department of Chemical Engineering, Indian Institute of Technology Guwahati, Guwahati 781039, Assam, India. E-mail: pugal@iitg.ernet.in

INTRODUCTION

Recently, polymer/layered inorganic nanocomposites (PLNs) have attracted great interest in the field of material chemistry because of their novel mechanical, thermal, and optical properties [1–5], which are mainly attributed to the high degree of dispersion of layered inorganic compounds in the polymer matrix. Among the PLNs, exfoliated PLN materials usually have molecular dispersion of high aspect ratio inorganic layers in polymer nanocomposites [6]. Several methods have been reported for the synthesis of the exfoliated nanocomposites with good properties such as melt intercalation, solvent blending, and in situ polymerization. In the case of the melt intercalation method, the melts of polymer and clay are directly blended in a screw extruder. This method is not suitable for samples with more than 20 wt% filler, and in the case of some polymers, the viscosity increases rapidly with the addition of a significant amount of nanofillers. In the case of the in situ polymerization method, the nanoscale clay particles are dispersed in a monomer or monomer solution and the resulting mixture is polymerized by any one of the standard polymerization methods. The main advantage is that the polymer is grafted onto the clay surface. The main concern of this method is the appropriate dispersion of the filler in the monomer. Sometimes it is required to modify the particle surface because settling is more rapid. Polymerization can be initiated either by heat or radiation, by the diffusion of a suitable initiator, or by an organic initiator. It has certain limitations, as this method is not economically suitable for the industrial preparation of polymer-clay nanocomposites due to its high cost, and as polymerization requires inert conditions and a highly pure monomer, initiators are needed. However, the solvent blending method overcomes some of the limitations of melt processing and in situ polymerization methods. Here the polymer and clay nanoparticles are dissolved and dispersed in solution. When the polymer and layered silicate solutions are mixed, the polymer chains intercalate and displace the solvent within the interlayer of the silicate. Upon solvent removal, the intercalated structure remains, resulting in polymer nanocomposites [7].

Montmorillonite is a clay commonly used for making polymer nanocomposites. Its layer structure is constructed of an octahedral alumina sheet sandwiched between two tetrahedral silica sheets. Stacking of layers about 1 nm thick by a weak dipolar force leads to interlayer galleries. The galleries are normally occupied by cations such as Na^+, Ca^{2+}, and Mg^{2+}. Organomontmorillonite is obtained with a cation exchange reaction or the adsorption of small alkyl ammonium or other organic cations into the interlamellar spacings [8].

Several attempts to prepare polystyrene–clay nanocomposites have been reported. Friedlander and Grink [9] reported a slight expansion of

the 001 spacing of clay galleries by in situ polymerization and concluded that polystyrene was intercalated in clay galleries; Blumstein [10] questioned intercalation by polystyrene because he did not get any increase in the basal spacing. Later, Kato et al. [11] reported the intercalation of styrene into stearyl trimethyl-ammonium cation exchanged MMT. Akelah and Moet [12,13] have prepared polystyrene nanocomposites using acetonitrile as a solvent. They reported the intercalation in PS-clay nanocomposites, with a maximum basal spacing of 2.54 nm. Doh and Cho [14] prepared polystyrene-clay intercalated nanocomposites by the polymerization of styrene in the presence of organophilic clay. The intercalated polystyrene-clay nanocomposites exhibited better thermal stability than pure polystyrene. Sohn et al. [15] prepared polymer nanocomposites based on an organophilically modified montmorillonite (OMMT) and polystyrene (PS) by the solvent blending method using chloroform as a cosolvent. Formation of intercalation nanocomposites was confirmed from the increase in interlayer spacing. The reactive cationic surfactant, vinyl benzyl di-methyl dodecyl ammonium chloride (VDAC), was used for ion exchange with sodium ions in MMT. Then exfoliated polystyrene-clay nanocomposites were prepared by direct dispersion of organophilic MMT in styrene monomer followed by free radical polymerization [16]. Uthirakumar et al. [17] prepared the exfoliated polystyrene (PS)/clay nanocomposites via in situ polymerization using a cationic radical initiator-intercalated montmorillonite hybrid. The exfoliated structure resulted mainly due to the anchored radical initiator inside the clay galleries. Qiu et al. [18] prepared exfoliated PS/ZnAl LDH nanocomposites by a solution intercalation method. They reported that the thermal decomposition temperature of exfoliated PS nanocomposites was 16°C higher than that of pure PS. In another work, they have also developed exfoliated PS/LDH nanocomposites by emulsion polymerization [19]. The decomposition temperature of exfoliated PS/LDH sample with 5 wt% LDH was 19°C higher than that of pure PS when 50% weight loss was selected as a comparison point. Hong et al. [20] prepared PS/MMT nanocomposites by the free radical polymerization method. The nanocomposites showed about 9 and 3°C improvement in the thermal decomposition temperature and glass transition temperature, respectively, over pure PS. The extensive literature review suggests that very few works have been reported on the fabrication of PS/MMT nanocomposite by solvent blending method. In particular, no research work on the influence of the processing conditions (nanomaterial loading, refluxing time and refluxing temperature) on the properties of PS/OMMT nanocomposites derived via solvent blending method has been studied before.

This work addresses the preparation of PS/OMMT nanocomposites by solvent blending method. The influence of operating conditions such as nanomaterial (OMMT) loading, refluxing time, and refluxing temperature

on the structural and thermal properties of PS nanocomposites is also investigated.

EXPERIMENT

Materials

Polystyrene supplied by National Chemicals, Vadodara, India and organically modified clay, CRYSNANO-1010 supplied by Crystal Nanoclay Private Limited, India, were used throughout this work. Xylene procured from Merck, India was used as received without further purification.

Preparation of Nanocomposites

PS/OMMT nanocomposites were prepared by the solvent blending method in which xylene was used as a solvent. A known quantity of OMMT was added to xylene with continuous stirring for 24 h at the desired temperature until the OMMT was completely dispersed. After that, desired quantity of PS added into the above OMMT solution and refluxed for the desired time at the same temperature. Then it was spread over a glass plate and left for 12 h in ambient temperature yielding a viscous gel layer. Finally, the film was heated in an oven for 6 h at 100°C to remove the remaining solvent to obtain PS/OMMT nanocomposites. The prepared nanocomposite films were characterized for structural and thermal properties. The pure PS film was also prepared by an identical procedure in the absence of OMMT. To study the effect of nanomaterial loading, various PS/OMMT nanocomposites were prepared with 5, 7, 20 wt% of OMMT (relative to PS) at constant temperature (25°C) and refluxing time (12 h). Similarly, the effect of refluxing time and temperature on the properties of nanocomposites was studied for a constant nanomaterial loading (5 wt%). The conditions used to prepare PS nanocomposites using CRYSNANO-1010 nanomaterial were presented in Table 1.

Table 1: Processing conditions for PS/OMMT (CRYSNANO-1010) samples.

Name of sample	OMMT content (wt %)	PS content (wt %)	Temperature (°C)	Refluxing time (h)
#PSNC1010 (20, 25, 12)	20	80	25	12
PSNC1010 (7, 25, 12)	7	93	25	12
PSNC1010 (5, 25, 12)	5	95	25	12
PSNC1010 (5, 25, 6)	5	95	25	6
PSNC1010 (5, 110, 6)	5	95	110	6

#(20, 25, 12) represents nanomaterial loading (wt %), refluxing temperature (°C), and refluxing time (h), respectively.

MEASUREMENTS

X-ray diffraction (XRD) profiles of OMMT and various PS/OMMT nanocomposite samples were recorded under air at room temperature using the AXS D8 ADVANCE Fully Automatic Powder X-Ray Diffractometer (Bruker) equipped with a Cu Kα radiation ($\lambda = 0.15418$ nm) and Ni filter. The patterns were acquired for 2θ range of 2^o to 50^o with a scan speed of $0.05^o\,s^{-1}$. The transmission electron microscopy (TEM) images were obtained on a JEOL JEM-2100 transmission electron micro analyzer with an accelerating voltage of 200 KV. The morphology and composition (EDX) of PS/OMMT nanocomposites were analyzed by scanning electron microscopy (SEM) on a variable Pressure Digital Scanning Electron Microscope (model LEO 1430 VP) operating at an accelerating voltage of 15 KV. The synthesized nanocomposites were analyzed using a Perkin Elmer Fourier transform infrared spectroscope (FTIR) to confirm the presence of OMMT in the PS/OMMT nanocomposites. The thermogravimetry (TG) analysis for thermal stability was performed under nitrogen atmosphere on a TGA/SDTA851e/LF/1100 model (Mettler Toledo) instrument using a heating rate of 10°C/min from 25 to 700°C for all the samples. Differential scanning calorimetry (DSC) was performed on a Mettler Toledo-1 series to evaluate the glass transition temperature (T_g) of the PS nanocomposites. Samples were heated from 25 to 200°C at a rate of 5°C/min under nitrogen atmosphere. The water uptake test was considered as a standard method to evaluate water resistance of the nanocomposite films using the gravimetric method. Water uptake of the nanocomposite films was determined by measuring the change in the weight before and after hydration. Five samples of each nanocomposite film (having dimensions 3 cm × 3 cm) were dried at 100°C for 4 h to bring each sample to an identical starting state. The nanocomposite samples were then weighed to note the dry weight. Finally, the dried samples were soaked in millipore water for 48 h. Then they were taken out, wiped with tissue paper and weighed immediately. The water uptake of the nanocomposite films was calculated using Eq. (1).

$$\text{Water uptake (wt \%)} = \frac{W_w - W_d}{W_d} \times 100 \tag{1}$$

where, W_w and W_d are the weights of wet and dry nanocomposite film, respectively.

RESULTS AND DISCUSSION

It was well-documented [18,21] that in the solvent blending method for making polymer nanocomposites, the processing conditions, such as nanomaterial loading, solvent used, refluxing time and refluxing temperature, play a major

role in determining the structure of the nanocomposites. In view of this, the influence of nanomaterial loading (OMMT), refluxing time and refluxing temperature on the properties of PS/OMMT nanocomposites were investigated in this work.

XRD Analysis

The XRD is an effective tool to characterize the types of the layered structure, that is, intercalated and/or exfoliated polymer/OMMT nanocomposites, because the peak changes with the gallery height of the OMMT. In the case of intercalated nanocomposites, the XRD peak is seen at larger d-spacing than in the pristine clay, whereas in the case of the exfoliated structure, no peak is seen. Figure 1 depicts the XRD patterns of PS, OMMT (CRYSNANO 1010), and PS/OMMT nanocomposites prepared with various nanomaterial loading. It can be seen that the basal spacing of d_{001} peak of the OMMT layers in the nanocomposites increases to 3.68 nm from 3.27 nm of the original OMMT layers, after refluxing for 12 h at 25°C with 5 and 7 wt% of nanomaterial loading. However, in the case of 20 wt% OMMT loading, the increment of the d_{001} value of the nanocomposite is 3.48 nm. It clearly suggests that the amount of intercalation of polymer into the clay galleries significantly depends on the nanomaterial loading. In all of the cases, OMMT layers in the nanocomposites have been intercalated, because a single extended polymer chain can penetrate between the silicate layers, and a well-ordered multilayer morphology

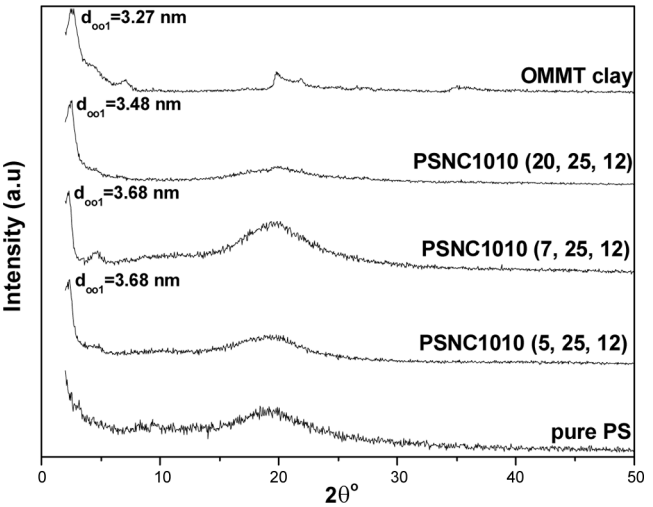

Figure 1: Effect of loading on the structure of PS/OMMT nanocomposites characterized by XRD.

results with alternating polymeric and inorganic layers. A similar observation was also obtained by Qiu et al. [18] for PS/ZnAl-LDH nanocomposites. In their study, the completely exfoliated PS/ZnAl nanocomposites were obtained by decreasing the LDH content to below 10 wt%.

The XRD patterns of PS, OMMT (CRYSNANO 1010), and PS/OMMT nanocomposites prepared with different refluxing times are shown in Figure 2. The basal spacing of d_{001} peak of the OMMT layers in the nanocomposites increases to 3.68 nm from 3.27 nm of the original OMMT layers, after refluxing for 6 and 12 h at 25°C with 5 wt% of nanomaterial loading. This confirms that OMMT layers in the nanocomposites are intercalated. However, there is no effect of refluxing time on the structure of nanocomposites studied in this work. A similar study was also carried out by Qiu et al. [18] for PS/ZnAl-LDH nanocomposites. They reported that the basal spacing of the LDH layers in the nanocomposites increased with refluxing time.

Figure 3 indicates the XRD patterns of PS, OMMT (CRYSNANO-1010), and PS/OMMT nanocomposites prepared with various refluxing temperatures. It is observed that the basal spacing of d_{001} peak of the OMMT layers in the nanocomposite increases to 3.68 nm from 3.27 nm of the original OMMT layers, after refluxing for 6 h at 25°C with 5 wt% of nanomaterial, which implies that the OMMT layer in the nanocomposite is intercalated. When the refluxing temperature increased to 110°C, the diffraction peak (001) completely disappears in the case of PSNC1010 (5, 110, 6) nanocomposite, which means that refluxing at high temperature can form an exfoliated

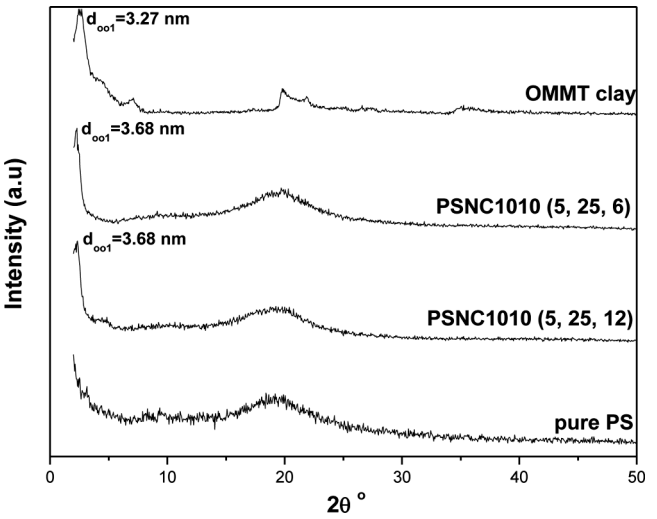

Figure 2: Effect of refluxing time on the structure of PS/OMMT nanocomposites characterized by XRD.

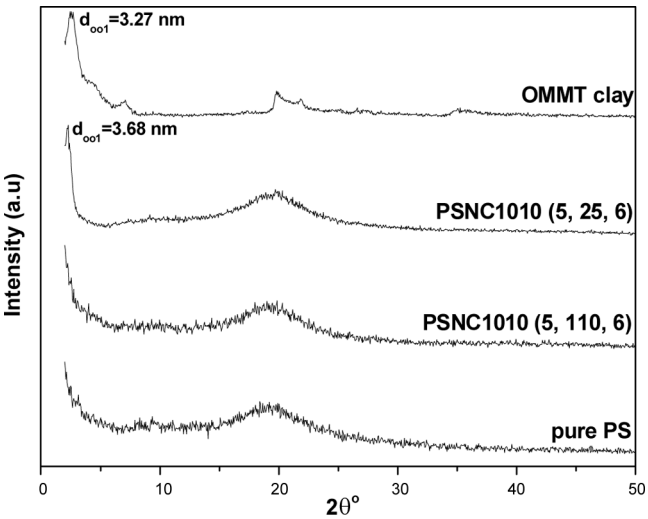

Figure 3: Effect of refluxing temperature on the structure of PS/OMMT nanocomposites characterized by XRD.

PS/OMMT nanocomposite, because the silicate layers are completely broken and uniformly dispersed in a continuous polymer matrix. The main reason for the development of the PS/OMMT nanocomposite structure from intercalated to exfoliated is that more and more OMMT layers broke into small fragments as the refluxing temperature increased, and thus form the exfoliated structure of nanocomposites. Qiu et al. [18] also achieved a similar type of completely exfoliated PS/LDH nanocomposites by increasing the refluxing temperature. Table 2 represents the complete XRD results of PS/OMMT nanocomposites.

FTIR Spectroscopy

FTIR technique has been used to identify the nature and symmetry of interlayer cations. The FTIR spectrum of OMMT (CRYSNANO-1010) is shown

Table 2: XRD results of pure OMMT and PS/OMMT (CRYSNANO-1010) samples.

Name of sample	2θ	d_{001} (nm)	Structure
Pure 1010	2.7	3.27	—
PSNC 1010 (20, 25, 12)	2.5	3.48	intercalated
PSNC1010 (7, 25, 12)	2.4	3.68	intercalated
PSNC1010 (5, 25, 12)	2.4	3.68	intercalated
PSNC1010 (5, 25, 6)	2.4	3.68	intercalated
PSNC1010 (5, 110, 6)	disappear	—	exfoliated

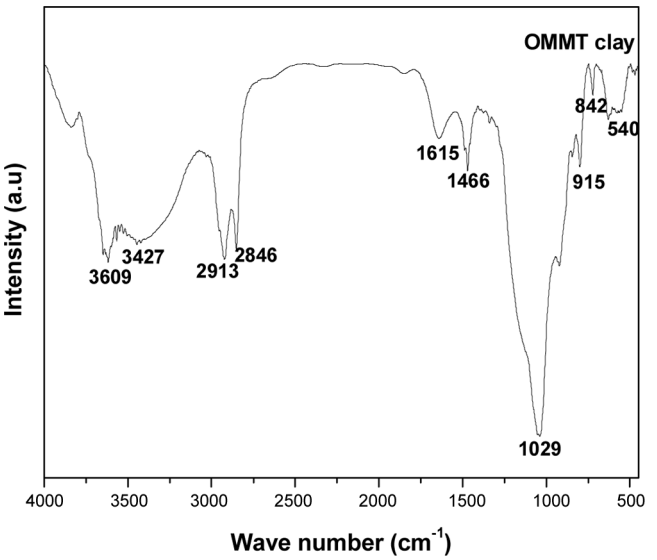

Figure 4: FTIR spectrum of OMMT (CRYSNANO-1010).

in Figure 4. The band has two features at 3609 cm^{-1} and at 3427 cm^{-1} showing the presence of two types of O-H groups: isolated OH groups and those involved in hydrogen bonding. The peaks at 2913, 2846, and 1466 cm^{-1} are for CH_2 asymmetric stretching, symmetric stretching, and in-plane scissoring vibrations, respectively, in the alkyl chains of the modifier used to make OMMT. The peak at 1615 cm^{-1} corresponds to the bending vibrational mode of hydrated water molecules and weakly bonded water molecules [22]. The band at 1029 cm^{-1} is attributed to the Si-O stretching vibration of OMMT. The bands observed at 540 and 456 cm^{-1} correspond to Al-O stretching and Mg-O bending vibrations of OMMT, respectively.

The pure PS (Figure 5) has several characteristic absorption bands at 3070 and 3030 cm^{-1} (aromatic C-H stretching vibration), 2960 and 2930 cm^{-1} (aliphatic C-H stretching vibration), 2000–1680 cm^{-1} (weak aromatic overtone and combination band), 1504 and 1496 cm^{-1} (C = C stretching vibration), 1453 and 1368 cm^{-1} (CH_2 bending vibrations), 757 and 698 cm^{-1} (CH out-of-plane bending of the phenyl ring or mono substituted benzene), and 540 cm^{-1} (out-of-plane deformation of the phenyl ring). The FTIR spectrum of the PS/OMMT nanocomposites shown in Figure 5 clearly exhibits the characteristic absorptions attributable to both the polymeric organic and inorganic groups. This indicates that the OMMT layers are dispersed into the PS matrix to form the PS/OMMT nanocomposite. Compared to pure PS, the PS/OMMT nanocomposite shows some new peaks in the region of 1029, 915, and 456 cm^{-1} corresponding to the Si-O stretching vibration, Al-O stretching, and Mg-O

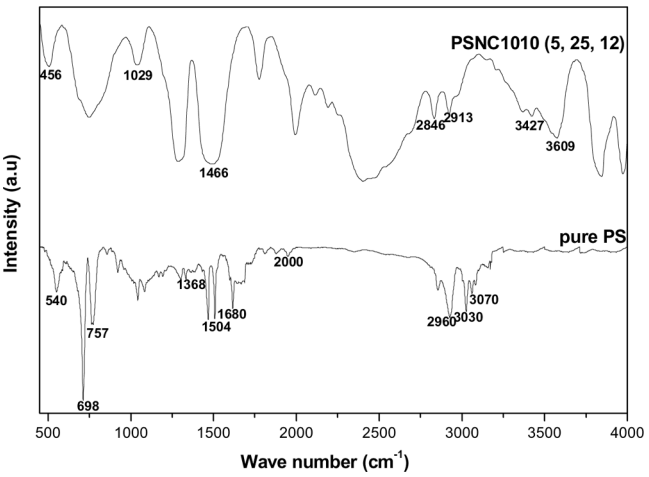

Figure 5: FTIR spectrum of pure PS and PS/OMMT (CRYSNANO-1010) nanocomposite.

bending vibrations of OMMT, respectively. These peaks indicate the existence of organically modified MMT in PS/OMMT nanocomposite. Similar types of results were also obtained for all other PS/OMMT nanocomposites (Figure 6) prepared with various nanomaterial loading.

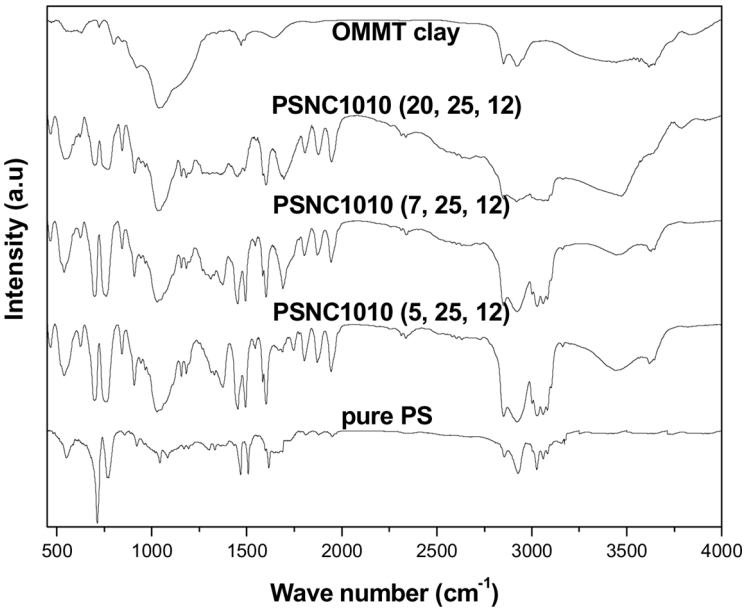

Figure 6: Effect of nanomaterial loading on the structure of PS/OMMT nanocomposites characterized by FTIR.

Scanning Electron Microscopy (SEM)

To directly reveal the state of clay dispersion in the polymer matrix, SEM images of PP/OMMT nanocomposites prepared via solvent blending method are provided. Figure 7 (a) presents the SEM image of exfoliated PS/OMMT nanocomposite (prepared with 5 wt% of OMMT loading at 110°C). In the case of exfoliated PS/OMMT nanocomposite, it is seen that the OMMT particle is smaller and the distribution of OMMT is more uniform with 5 wt% of nanomaterial loading. On the other hand, Figure 7 (b) shows the SEM image of PS/OMMT nanocomposite samples with 20 wt% nanomaterial loading. Apparently, this image shows that the size of the OMMT particle is large and the distribution of OMMT is uneven with small agglomeration. The composition of the PS/OMMT nanocomposites is also confirmed by EDX analysis (Figure 8). The presence of Si and Al atoms in EDX analysis reveals the presence of nanomaterial in the PS nanocomposite.

Transmission Electron Microscopy (TEM)

XRD analysis provides the information about the dispersion of clay. However, stronger evidences are needed for the judgment about a complete exfoliated structure. Cross-referencing XRD results with TEM study would provide a basis for a more objective analysis. The morphological structure of nanocomposites is further studied by the TEM analysis. Figure 9 (a) presents the TEM image of exfoliated PS/OMMT nanocomposite (prepared with 5 wt% of nanomaterial loading at 110°C). In the case of exfoliated PS/OMMT nanocomposite, it is observed that the OMMT layers (the dark part in Figure 9 (a)) are homogeneously dispersed with face-to-face orientations in the PS matrix (bright part). The photograph clearly shows the lamellar structure of OMMT exfoliated by the PS macromolecular chain; the lines of

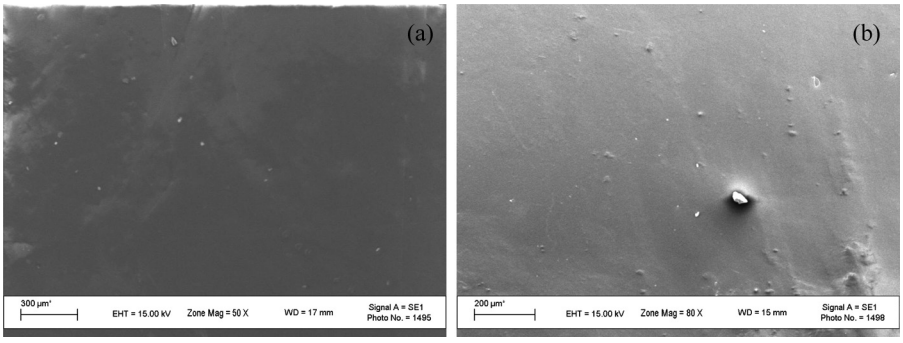

Figure 7: SEM images of PS/OMMT nanocomposites with different content of nanomaterial loading: a) 5 wt%, and b) 20 wt%.

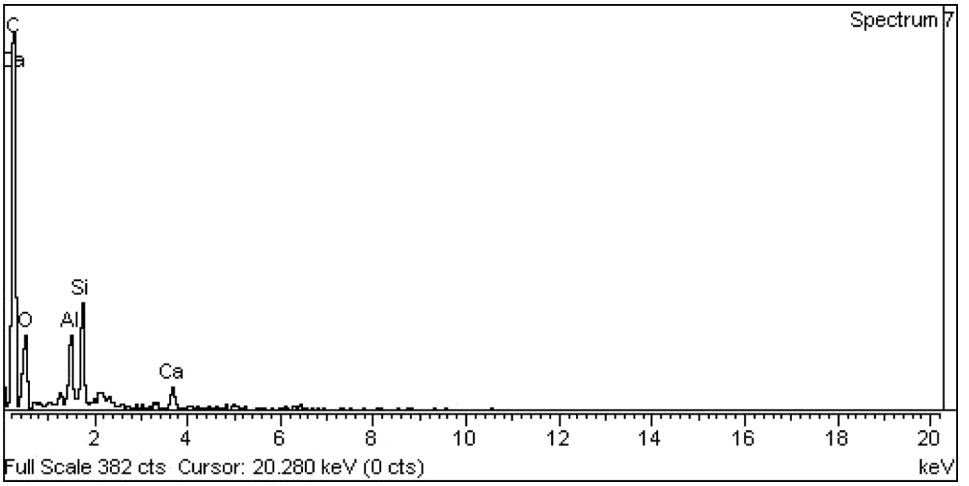

Figure 8: EDX analysis of intercalated PS/OMMT nanocomposites with 20 wt% of nanomaterial loading.

the layers are well shown using the arrow marks. The XRD result (Figure 3) also shows that the OMMT layers in the sample are completely exfoliated as mentioned above. So it is reasonable to describe this sample as exfoliated. On the other hand, Figure 9 (b) shows the TEM image of the PS/OMMT sample with 20 wt% OMMT loading. Apparently, this image shows an intercalated structure, which is in good agreement with the results reported from the XRD analysis [23].

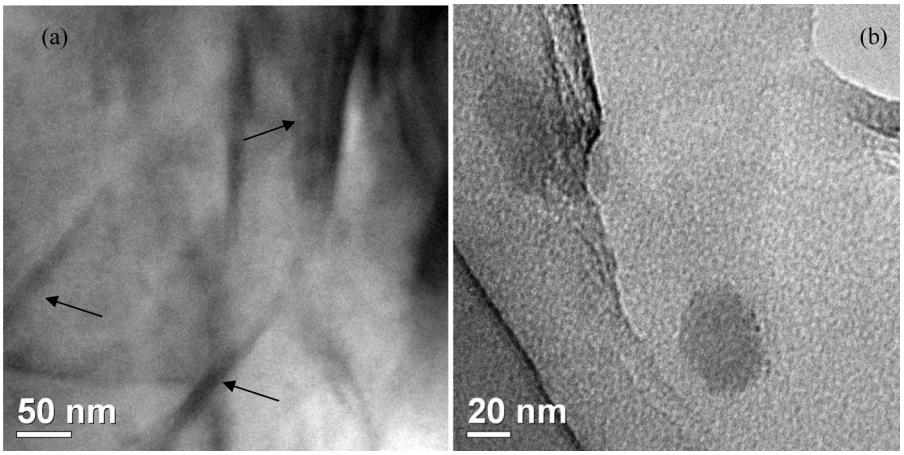

Figure 9: TEM images of PS/OMMT nanocomposites with various content of nanomaterial loading: (a) exfoliated (5 wt%), and (b) intercalated (20 wt%).

Thermal Properties

Thermogravimetric Analysis (TGA)

Figure 10 illustrates the TGA curves for pure PS, pure OMMT (CRYSNANO-1010) and PS/OMMT nanocomposites with various OMMT contents. The thermal decomposition of pure PS sample occurs in the range of 350–450 °C. Generally, the PS/OMMT samples exhibit two different types of weight losses. The first step of weight loss at about 150–350 °C is due to the evaporation of physically absorbed water and thermal decomposition of surfactant molecules present between the interlayer of OMMT. The second step of weight loss between 350–480 °C is attributed to the thermal degradation of PS chains and the formation of black charred residues. The degradation rate in this step is much slower compared to pure PS. This beneficial effect can be due to the hindered effect of OMMT layers for the diffusion of oxygen and volatile products throughout the composite material. After ~500°C, the curves all became flat and the inorganic residue mainly remained. When 15% weight loss is selected as a point of comparison, the thermal decomposition temperature for pure PS, PS/OMMT nanocomposite samples containing 5, 7, and 20 wt% of OMMT is determined as 393, 383, 372, and 375°C, respectively. It clearly demonstrates that the thermal decomposition temperature of nanocomposites is relatively lower than that of pure PS. The chemical (surfactant) used for modification of MMT is likely responsible for the initial destabilization of the nanocomposites. However, PS/OMMT nanocomposites show better thermal

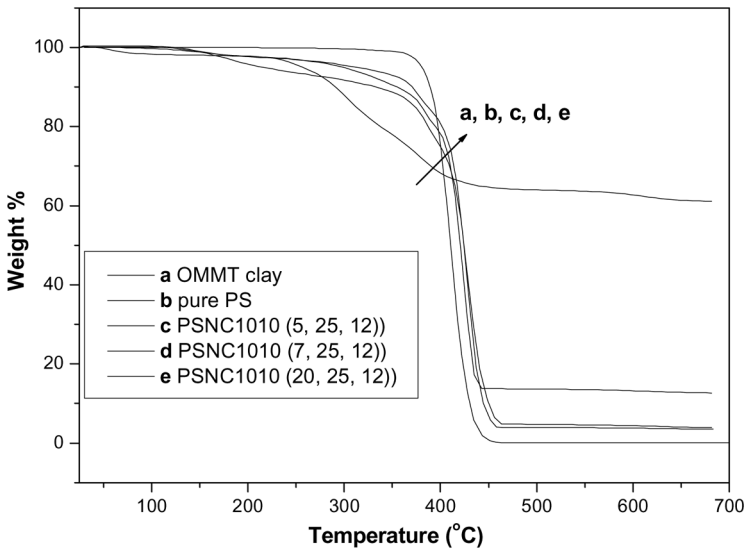

Figure 10: TGA curves of pure PS, pure OMMT, and PS/OMMT nanocomposites with various contents of OMMT.

stability at high temperatures (above 400°C), which is confirmed by the shifting of the TGA curve of PS/OMMT nanocomposites towards the right of the TGA curve for pure PS (see Figure 10). When 50% weight loss is selected as a point of comparison, the thermal decomposition temperature for pure PS, PS/OMMT nanocomposite samples containing 5, 7, and 20 wt% of OMMT is found to be 410, 424, 425, and 421°C, respectively. It can be seen that the thermal decomposition temperature of PS/OMMT nanocomposites is 11–15°C higher than that of pure PS, in which the PS/OMMT nanocomposite with 7 wt% has the best thermal stability. The excess loading of OMMT (for example 20 wt%), can make the nanocomposites decrease the thermal stability. The most probable reason is that the relatively large organic surfactant content of the composites produced less stable charred layers during the decomposition [24]. Very similar behavior has already been observed in some polymer/silicates [1,25] and polymer/LDH [18] nanocomposites. In the work of Qiu et al. [18], they showed that the thermal decomposition temperature of PS/ZnAl-LDH nanocomposites was 16°C higher than that of pure PS. A similar observation is also deduced from the first TGA derivative for PS nanocomposites illustrated in Figure 11. The peak indicates the temperature (T_{max}) at a maximum rate of degradation. The entire first TGA derivative curves for PS nanocomposites are shifted towards the right side of pure PS, indicating higher thermal stability. The maximum degradation temperature for pure PS is 413°C but that of the PS/OMMT nanocomposite is 432°C, indicating a 19°C improvement with just 7 wt% of OMMT loading. Therefore, an improvement in the thermal stability will lead to better service performance of the nanocomposites at an elevated temperature. Similar results have also been observed by other researchers [14,17].

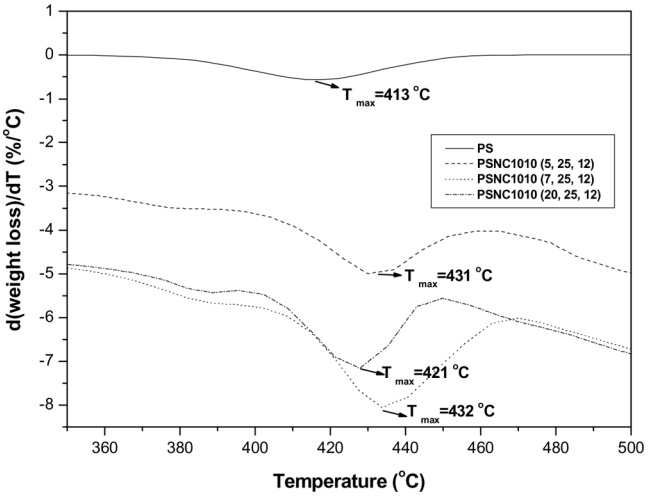

Figure 11: TGA derivative of pure PS and PS/OMMT composites with various OMMT contents.

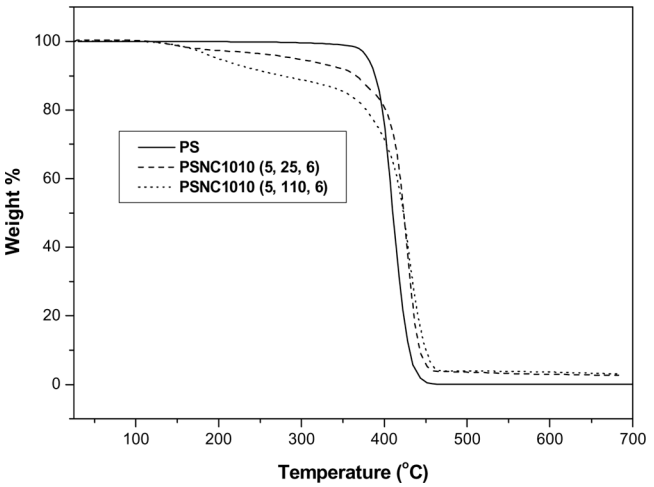

Figure 12: TGA profiles for pure PS and PS/OMMT nanocomposites prepared at different refluxing temperatures.

Figure 12 presents the TGA curves of the PS/OMMT nanocomposites prepared with various refluxing temperatures. Nanocomposite prepared at 110°C (PSNC1010 (5, 110, 6)) has higher thermal decomposition temperature than that of the nanocomposites prepared at 25°C (PSNC1010 (5, 25, 6)). When 50% weight loss is selected as a point of comparison, the thermal decomposition temperature for the PSNC (5, 110, 6), and PSNC (5, 25, 6) is 425 and 420°C, respectively. The different thermal behaviors can be explained by the different proportion of exfoliated and intercalated structures in these nanocomposites. The amount of exfoliated OMMT layers in PSNC1010 (5, 25, 6) is not sufficient to promote significant improvement of the thermal stability because many of the OMMT exist as intercalated structures in this sample. Increasing refluxing temperature to 110°C leads to relatively more exfoliated OMMT layers, which increased the thermal stability of the nanocomposites. These results suggest that the thermal stability of the exfoliated nanocomposites is better than that of intercalated composites. A similar observation is also deduced from the first TGA derivative of PS composites illustrated in Figure 13, where the peak indicates the temperature (T_{max}) at a maximum rate of degradation, delayed at a higher temperature. The TGA results for pure PS and PS/OMMT nanocomposites are given in Table 3.

Differential Scanning Calorimetry (DSC)

To investigate the mobility of PS chains in terms of its T_g (glass transition temperature) in the clay layers, DSC study of pure PS and PS/OMMT

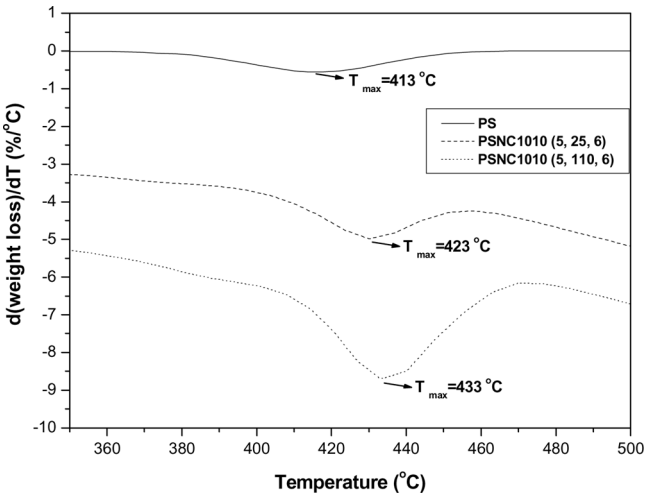

Figure 13: TGA derivative of pure PS and PS/OMMT composites prepared at various refluxing temperatures.

nanocomposites has been carried out and the results are reported in Figure 14. The glass transition temperature is determined at the inflection point between the onset and the end-set temperatures. The T_g of the composites is remarkably increased relatively to the neat polystyrene, but slightly as the OMMT content increases. This is clearly caused by the strong interaction between OMMT and PS, which limits the cooperative motions of the PS main chain segments [26]. The T_g of pure PS, PS/OMMT nanocomposites samples containing 5, 7, and 20 wt% of OMMT is determined as 69.0, 74.1, 74.5, and 75.2°C, respectively. It is observed that the glass transition temperature of PS/OMMT nanocomposites is 5.0–6.2°C higher than that of pure PS. The improvement in the T_g is due to the silicate nanoplatelets with high aspect ratios in the PS matrix, since the segmental motions of the polymer chains are restricted at the organic–inorganic interface, due to the confinement of the PS chains between the silicate layers as well as the silicate surface-polymer interaction

Table 3: TGA results for pure PS and PS/OMMT (CRYSNANO-1010) samples.

Name of sample	Temperature at 15 wt% degradation in °C (T_{15})	Temperature at 50 wt% degradation in °C (T_{50})	ΔT_{50} (°C)
Pure PS	393	410	—
PSNC1010 (20, 25, 12)	375	421	11
PSNC1010 (7, 25, 12)	372	425	15
PSNC1010 (5, 25, 12)	383	424	14
PSNC1010 (5, 25, 6)	386	420	10
PSNC1010 (5, 110, 6)	354	425	15

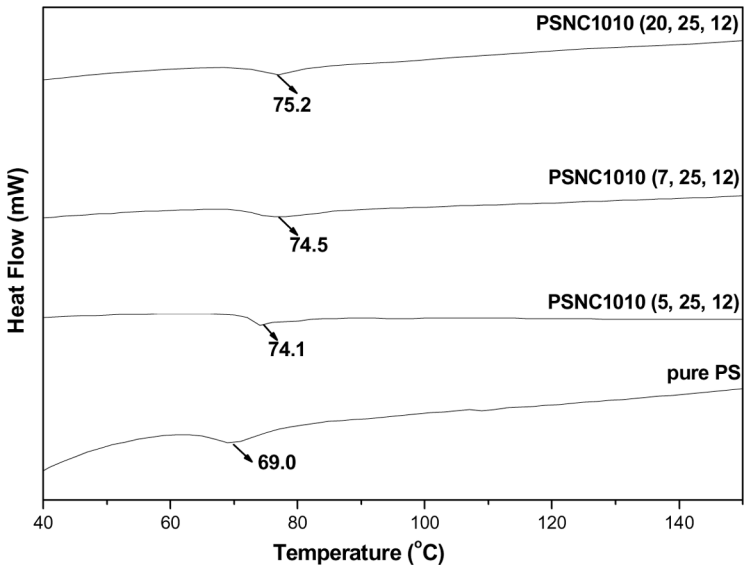

Figure 14: DSC curves of pure PS and PS/OMMT composites with various OMMT contents.

in the nanostructured hybrids. Noh et al., also reported an improvement of ~5°C in the T_g of PS/MMT nanocomposites containing 30 wt% of MMT prepared by emulsion polymerization [27]. The majority of the other well-dispersed polymer/clay nanocomposites also exhibited higher T_g than their corresponding pristine polymers [28,29].

Water Uptake Test

The prepared PS/OMMT nanocomposite films are tested for water uptake capacity and the results are reported in Table 4. The water uptake capacity of the nanocomposites is decreased in comparison to pristine PS. The water uptake of pure PS film is found to be 2.20 wt%, while the water uptake of

Table 4: Water uptake capacity of pure PS and PS/OMMT (CRYSNANO-1010) samples.

Name of sample	Water uptake (wt %)
Pure PS	2.20
PSNC1010 (20, 25, 12)	0.69
PSNC1010 (7, 25, 12)	0.87
PSNC1010 (5, 25, 12)	0.98
PSNC1010 (5, 25, 6)	1.10
PSNC1010 (5, 110, 6)	0.82

PS/OMMT nanocomposite becomes 0.69 wt%. The hydrophilicity of OMMT is drastically reduced due to the effect of two influences: its treatment with the inorganic ions between the galleries by organic ions (surfactants) has displaced the outer and inner hydration shells that are coordinated to the inorganic cations, and the presence of PS chains in the interlayer space [30]. From these data, we can conclude that the water uptake is negligible in the case of PS/OMMT nanocomposites. Hence these nanocomposites are very much useful in preparing waterproof ink and paint.

CONCLUSIONS

Intercalated/exfoliated polystyrene/organomontmorillonite (PS/OMMT) nanocomposites have been synthesized via the solvent blending method. The influence of operating conditions such as nanomaterial (OMMT) loading, refluxing time, and refluxing temperature on the structural and thermal properties of PS nanocomposites is also studied. The XRD and TEM results confirm the formation of intercalated/exfoliated PS/OMMT nanocomposites. The FTIR, SEM, and EDX results confirm the presence of nanomaterial in PS/OMMT nanocomposites. Completely exfoliated nanocomposites can be achieved by increasing the refluxing temperature. The TGA profiles of PS/OMMT nanocomposites show a significantly enhanced thermal stability compared with pure PS. The PS/OMMT nanocomposite with 7 wt% OMMT has the best thermal stability and its thermal decomposition temperature is 15°C higher than that of pure PS. The DSC profiles of PS/OMMT nanocomposites show a significantly enhanced glass transition temperature compared with pure PS. The glass transition temperature of PS/OMMT nanocomposites is about 5.0–6.2°C higher than that of pure PS. The water uptake capacity of PS/OMMT nanocomposites is negligible when compared with pure PS.

REFERENCES

[1] Alexandre, M., and Dubois, P. *Mater. Sci. Eng. R.* **28**, 1 (2000).

[2] Kim, Y. K., Choi, Y. S., Wang, M. H., and Chung, I. J. *Chem. Mater.* **14**, 49 (2002).

[3] Vyazovkin, S., Dranca, I., Fan, X. W., and Advincula, R. *Macromol. Rapid Commun.* **25**, 498 (2004).

[4] Lu, J., and Zhao, X. P. *Coll. Interf. Sci.* **273**, 651 (2004).

[5] Chen, G. X., Choi, J. B., and Yoon, Y. S. *Macromol. Rapid Commun.* **26**, 183 (2005).

[6] Choi, Y. S., Choi, M. H., Wang, K. H., Kim, S. O., and Chung, I. J. *Macromolecules* **34**, 8978 (2001).

[7] Chen, W., Feng, L., and Qu, B. J. *Solid State Commun.* **130**, 259 (2004).

[8] Chen, G., Han, B., and Yan, H. *Coll. Interf. Sci.* **201**, 158 (1998).

[9] Friedlander, H. Z., and Grink, C. R. *Polym. Sci. Polym. Lett.* **2**, 475 (1964).

[10] Blumstein, A. *Polym. Sci. Part A.* **3**, 2653 (1965).

[11] Kato, C., Kuroda, K., and Takahara, H. *Clay and Clay Miner.* **29**, 294 (1981).

[12] Akelah, A., and Moet, A. *Mater. Sci.* **31**, 3189 (1996).

[13] Akelah, A., and Moet, A. *Mater. Lett.* **18**, 97 (1993).

[14] Doh, J. G., and Cho, I. *Polym. Bull.* **41**, 511 (1998).

[15] Sohn, J. I., Lee, C. H., Lim, S. T., Kim, T. H., Choi, H. J., and John, M. S. *Mater. Sci.* **38**, 1849 (2003).

[16] Fu, X., Tajuddin, Y., and Qutubuddin, S. (1998). *AIChE Annual Meeting*, Miami, FL.

[17] Uthirakumar, P., Song, M. K., Changwoon, N., and Lee, Y. S. *Europ. Polym. J.* **41**, 211 (2005).

[18] Qiu, L., Chen, W., and Qu, B. *Polym. Degrad. Stab.* **87**, 433 (2005).

[19] Qu, B., and Qiu, L. *Coll. Interf. Sci.* **301**, 347 (2006).

[20] Hong, H., Ding, C., Guo, B., He, H., and Jia, D. *Europ. Polym. J.* **41**, 1781 (2005).

[21] Wang, H. W., Chang, K. C., Yeh, J. M., and Joeliou, S. *Appl. Polym. Sci.* **91**, 1368 (2004).

[22] Manoratne, C. H., Rajpakse, R. M. G., and Dissanayake, M. A. K. L. *Int. J. Electrochem. Sci.* **1**, 32 (2006).

[23] Triantafillidis, C. S., LeBaron, P. C., and Pinnavaia, T. J. *Chem. Mater.* **14**, 4088 (2002).

[24] Chen, W., and Qu, B. J. *Mater. Chem.* **14**, 1705 (2004).

[25] Paul, M. A., Alexandre, M., Degee, P., Henrist, C., Rulmont, A., and Dubois, P. *Polym.* **44**, 443 (2003).

[26] Huang, J. C., Zhu, Z., Yin, J., Qian, X., and Sun, Y. Y. *Polym.* **42**, 873 (2001).

[27] Noh, M. W., and Lee, D. C. *Polym. Bull.* **42** (5), 619 (1999).

[28] Fu, X., and Qutubiddin, S. *Polym.* **42** (2), 807 (2001).

[29] Zidelkheir, B., Boudjemaa, S., Abdel Goad, M., and Djellouli, B. *Iranian Polym. J.* **15**, 645 (2006).

[30] Morgan, A. B., and Harris, J. D. *Polym.* **45**, 8695 (2004).